Chapter 2

Literature Review

2.1. Introduction

After the Discovery of graphene from graphite in 2004, scientists are attracted much intention in the field of nanomaterial science especially in carbon based nano material due to their potential applications in both science and technology. There are different forms of graphene-based materials exist in nature. They are graphene oxide (GO), reduced graphene oxide (RGO), functionalized graphene oxide, exfoliated graphite, functionalised reduced graphene oxide and graphene quantum dots (GQD) have been synthesised reliably in high scale for the interest of research as well as application in the different field. It has been demonstrated that graphene-related materials as suitable candidate for incorporation into a variety of functional materials due to excellent properties of graphene together with the ease of processibility and functionalization. So, this novel graphene based nano material has become one of the popular research area in nanomaterial science due to their unique optical and mechanical properties with different applications in various field [1-7]. As, we have focused our research on the luminescence property of graphene based material and therefore, it is need to know about graphene, graphene based material and the origin of photoluminescence of graphene based material. Hence, we will highlight the latest literature report in this chapter such as the brief invention history of graphene, structure and property of graphene, different method of synthesis of graphene, graphene polymer composite material, photoluminescence (PL) of graphene based material and application of photoluminescence of graphene based material.

2.1.1. Historical Background of Invention of Graphene

In the year of 1859, B. C. Brodie, a British professor named Graphon' for oxidized graphite flake [8]. He oxidised graphite flake by mixing potassium chlorate, fuming nitric acid and produced graphite oxide. The used chemicals are very dangerous for the oxidation of graphite and prone to explosion. Kohlschütter et al reported the properties of graphite oxide flake in 1918 [9] and they solved the structure of graphite oxide flake by measurements of single-crystal diffraction in 1924 [10]. The idea of graphene was introduced for the first time in 1947 by Canadian physicist P. R. Wallace [11]. He measured the electrical conductivity by theoretical calculations. He did not use the term, “graphene” in his report, instead, he just termed as “single hexagonal layer”. In 1948, G. Ruess and F. Vogt detected few layer graphite through their transmission electron microscopy (TEM) images [12]. Hummers and Offeman

has reported a efficient and better method for the preparation of graphite oxide in 1957.They used the chemicals for the oxidation of graphite are sulfuric acid, sodium nitrate and potassium permanganate [13]. In 1962, first time Hanns-Peter Boehm synthesised a single-layer graphite sheets [14]. The word ‘graphene’ first used to represent the single sheets of graphite as a constituent of graphite intercalation compounds in 1987 [15]. In 2004, A. Geim and K. Novoselov isolated monolayer graphene sheets from bulk graphite via micromechanical cleavage or Scotch tape technique [1] and awarded Nobel Prize in 2010.

Year	**Invention**
1859	B. C. Brodie synthesizes graphite oxide and introduces the word ‘Graphon’
1918	Properties of graphite oxide flakes are described
1924	Structure of graphite oxide is identified
1947	P. R. Wallace introduces the theory of graphene
1948	Few-layer graphite is detected by G. Ruess and F. Vogt using TEM
1957	Hummers and Offeman invent a new method for graphite oxide synthesis
1962	Single-layer graphite sheets are identified
1987	The name ‘Graphene’ has introduced
2004	A. Geim and K. Novoselov isolate single-layer graphene sheets from bulk

2.2. Structure of Graphene and Graphene Oxide (GO)

Graphene is basically a single sheet of a graphitic lattice. The two dimensional arrangement of the sp2 hybridised carbon atom has densely packed honeycomb shaped lattice structure in which each unit cell is made of two atoms with carbon-carbon distance 0.142 nm.[Fig. 1] In graphene, 2*s* and 2*p* electrons participates in hybridisation and form three sp2 orbitals, leaving a pure *p*-orbital. The sp2 orbitals are oriented in a plane at 120^{o} angles, and thus the lattice formed which looks like a honeycomb (hexagonal) shape. The σ and σ* states are formed by three sp2 orbitals within the three neighbouring carbon atoms and the delocalised π and π* states are introduced by the remaining *p*-orbital. These π and π* states introduced valance and conduction bands within the graphene material [16].

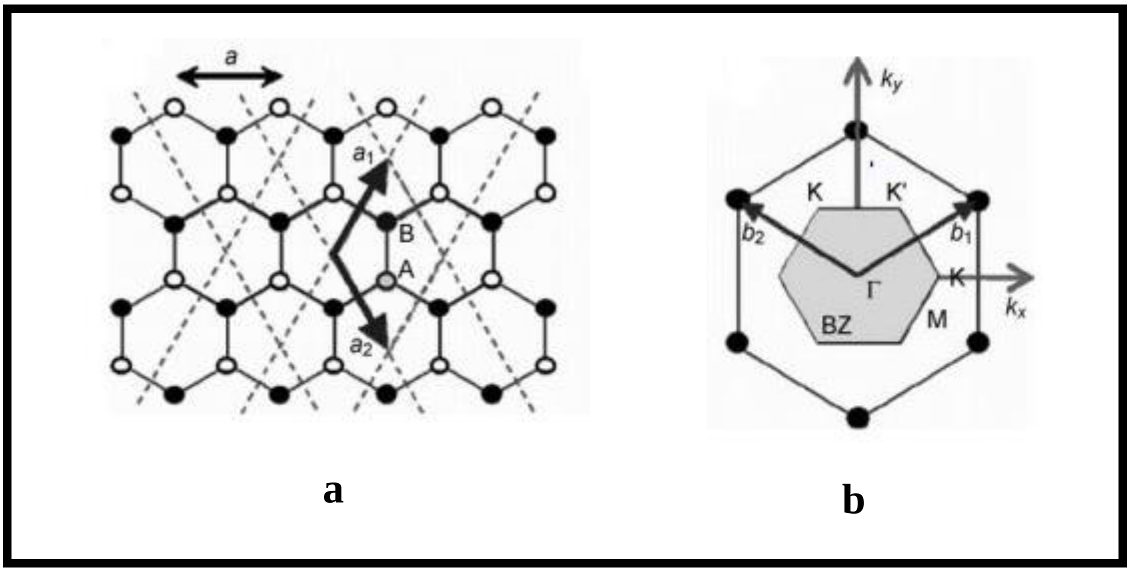

Fig. 1 Structure of Graphene

.

The chemically functionalised and oxidised form of graphene is known as GO. This is also a sheet of carbon atoms consists of oxygen containing functional groups either on the edges or on the surface of the GO [Fig. 2]. The carbon atoms (50-60%) of GO formed covalent bond with oxygen to form epoxy groups and hydroxyl and thereby sp3 hybridized structure is observed [17-18].

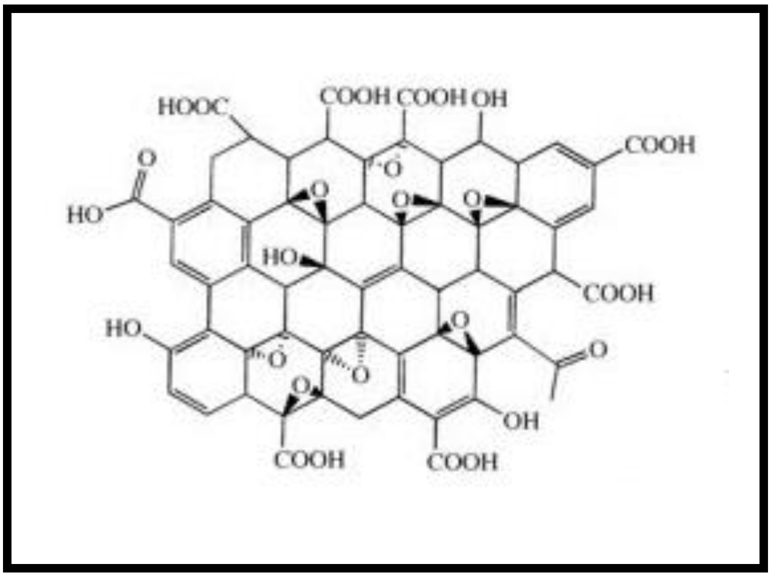

Fig. 2 Structure of Graphene Oxide

The remaining carbon atoms in GO bonded to the neighbouring carbon and also bonded to the carboxyl or carbonyl groups with oxygen through sp2 hybridization. The edges of graphene sheet contain most of the carboxyl and carbonyl groups. Therefore, two dimensional array of GO is a mixture of both sp2 and sp3 hybridized carbon atoms.

2.3. Properties of Graphene

Graphene is an exciting novel material due to its extraordinary optical, electronic and thermal properties, mechanical properties and helps to the researcher to apply in the different area of science and technology. Listed here are a few excellent graphene properties.

2.3.1. Mechanical strength

One of the remarkable property of graphene is the inherent strength due to the long carbon bond strength. It is a powerful material with a tensile strength of 1.3 x 1011 Pa and also a very lightweight and thinnest material with a value of 0.77 milligrams per square meter. The mechanical strength of graphene is incomparable and it can enhance significantly the strength of many composite materials [19-21].

2.3.2. Flexibility and elasticity

Graphene is actually very strong and also stronger than diamond. The strong bond is formed in a hexagonal pattern by the repetition carbon atoms of sp2 hybridized in graphene with the other carbon atoms. This makes graphene to exhibits its flexibility. When it comes to elasticity, it has been found that the spring constant value is between 1-5 Nm-1, with a Young's modulus of 0.5 TPa [20-31].

2.3.3. Impermeability

Graphene is the flattest and the thinnest material. The sp2 hybridized carbon atoms are connected to each other and formed a two dimensional (2D) honeycomb lattice structure with large electron density in its aromatic benzene rings and it does not allow any molecules to pass through the lattice of hexagonal structure [22-23].

2.3.4. Electronic properties

Graphene is a zero band gap semi metal having unique electrical properties. The graphene offers moderately less resistance to the electrons due to its unique structure and it can move easily. Therefore, the transportation of electric current in graphene is much better than the good conductors like copper .The electrons in graphene has longer mean free path compared to other materials. The excellent conductivity of graphene because of the delocalized pi- electrons in the hexagonal lattice [24].The overlapping of pi orbitals increases the strength of the C-C bonds in graphene. The bonding and antibonding of these pi orbitals are mainly responsible for the outstanding electronic properties of graphene [25]. Thus, unique electrical property of graphene makes a promising candidate for the manufacturing of nanoelectronic devices.

2.3.5. Optical properties

The graphene is thinnest ans also a transparent material that transmits about 97-98% of light incident on it [26]. It absorb white light (2.3%) in spite of having one atom thickness. Graphene is a zero band gap semiconductor which has high electrical conductivity and electron mobility [27]. In the visible region, each layer of graphene absorbs up to 2.3% of white light having reflectance of less than 0.1%.The absorption also depends on the the number of stacked layers one after the other. When, the input value of optical intensity is greater than the threshold value (known as the saturation fluence), the unique absorption is saturated and this is known as saturable absorption. Thus, it has wide range of applications in ultrafast photonics as well as in fiber lasers [28].

2.3.6. Thermal properties

The versatile thermal properties of graphene because of its sp^2 hybridized covalent bonding between the carbon atoms makes a interest in the field of heat transfer physics, which paves the way of application in thermal management [29]. Graphene exhibits an excellent heat conductor property than silver and copper and makes a promising material for thermoelectric applications.

2.4. Method of Synthesis of Graphene

After the discovery of graphene in 2004, different methods have been developed for the synthesis of graphene and its derivatives. Among the various method, top down method and bottom up method are the effective method to synthesis of graphene.

2.4.1. Top Down Method

The top down method includes Hummers method and modified hummers method, which is the most common method of synthesis of graphene oxide. The top-down approach is a process of slicing or successive cutting of a bulk material like graphite by means of oxidation, intercalation, and/or sonication to get nano sized particles. The major advantages of top down approach are high yield, solution based process ability, cost efficiency and ease of implementation. However, top-down method has more defects compared to bottom-up method. Still now, there are several reliable top- down method have been developed to synthesis of defect-free and high quality graphene. The top down method includes hummers method and modified hummers method, which is the most common method of synthesis of graphene oxide (GO). The others top down methods are electrochemical exfoliation of graphite [30], mechanical exfoliation of graphite [31], reduction of graphene oxide and thermal exfoliation [32]. The most simple way and cost effective process for the production of graphene is the reduction of graphene oxide which has been synthesised by modified Hummers method. The synthesis of graphene by reduction of GO allowing the preparation of graphene nanocomposites as the produced graphene is a hydrophilic graphene materials. However, it is reported that the conductivity of graphene sheets produced by using Chemical vapour deposition (CVD) method has higher than the RGO produced by reduction of GO. The Hummer and Staudenmaier methods are the common methods of way to prepare GO and then graphene from GO which involves the oxidation of graphite and the produced GO contains hydrophilic groups on its surface. In Hummer's method, potassium permanganate ($KMnO_4$), sulfuric acid (H_2SO_4) and sodium nitrate (NaNO3) are used to oxidize graphite [33] while Brodie and Staudenmaier used the combination of potassium chlorate ($KClO_3$) and nitric acid (HNO_3) to oxidise graphite [34]. One-or multi-layer Graphene oxide (GO) sheets are produced through ultra-sonication after the oxidation of graphite. Graphene-like sheets may be produced from GO by increasing the conjugation via removal of the oxygen containing functional groups through reduction. The preparation of pure graphene from GO is still a challenge. The presence of remaining functional groups after reduction and reduction induced defects produces a new kind of materials different from pure graphene and GO.

Although, this new material is commonly known as chemically derived graphene, also named as reduced graphene oxide (rGO), chemically converted graphene, functionalized graphene, or reduced graphene.

2.4.1.1. Hummers Method

According to hummers method ,Graphene oxide (GO) was synthesized by using graphite flakes and others chemicals like sodium nitrate, hydrogen peroxide(30%), sulphuric acid(70%), potassium permanganate (99%),. KMNO4 (9g) was added slowly to the solution of concentrated H_2SO_4 (69ml) containing graphite (3g) and $NaNO_3$ at different proportions at 0^0C. Now, the mixture was stirred at room temperature for 5 days and then distilled water added slowly to mixture at the temperature below 98^{o}C for 3 hrs. Then, yellow suspension diluted and solution of H_2O_2 was added drop wise. Now the obtained reaction mixture was centrifuged and washed. After vigorous washing, graphene oxide collected and dried by vacuum at 50^{o}C. Reduced graphene oxide likely graphene produced by using graphene oxide (75mg) which was dispersed in water (75ml) by sonication and then sodium borohydride (600 mg) was added to the graphene oxide dispersion and pH adjusted to 9-10 by using 5% sodium carbonate solution. Now, the mixture is under the constant string for 1 hour at 80^{o}C and then the dispersion becomes black in colour. Then, the product is centrifuged at 10000 rpm for 15 min and washed 3-4 times with distilled water to remove all the impurities. Thus finally graphene is prepared [35-38]. The Hummer's method has tremendous attention to the researcher for the preparation of GO sheets from graphite due to its low cost, easy access, and application in different field .However, higher defects as and disorders in the graphene oxide along with electrically insulating nature of GO are major drawbacks of this method. In this method, the exfoliation of graphite flake/graphite powder by oxidation chemically and producing graphene sheets which creats steric hindrance and affect the π- stacking interaction between the graphene sheets. Thus, the graphene oxide sheets are nearly insulating in nature.

Hence, the different properties particularly in respect of applications in electronics of graphene sheets should be non-achievable. Therefore, it is very important to reduce GO as it restores the conductivity of the GO sheets .There are several method in the literature like chemical reduction, thermal reduction etc has been used for reduction of the graphene oxide sheets and has been discussed in below.

2.4.1.2. Modified Hummer Method

According to Kovtyukhova, an additional pre-oxidation step is involved in this method as compared with hummer method. He reported that this peroxidation step was important to terminate the formation of incompletely oxidized graphite particle. According to this method, the graphite flake is pre-oxidized by using the chemicals like concentrated H_2SO_4, $K_2S_2O_8$ and P_2O_5. Then pre-oxidized graphite flake is further oxidized using hummers method [36]. The washing process involved simple decantation and centrifugation technique at 5000 rpm for 30min which result in formation of graphene oxide [39].

2.4.1.3. Chemical Reduction of GO

Graphene produced by using reduction of graphene oxide (75mg) which was dispersed in water (75ml) by sonication and then, added sodium borohydride (600 mg) to the graphene oxide (GO) dispersion and adjusted pH to 9-10 by using 5% sodium carbonate solution. Now, the mixture is under the constant string for 1 hour at 80^{o}C and then the dispersion becomes black in colour. Then, the product is centrifuged around at ten thousand rpm for 15 min and to remove all the impurities, it was washed 3-4 times by distilled water. Thus finally graphene is prepared [38].

2.4.1.4. Thermal reduction method

GO is heated rapidly at very high temperature under inert atmosphere in this method and leads to the exfoliation of GO. After reduction, it produces reduced GO sheets [40]. CO2 gas evolves when GO was heating. It is due to the decomposition of epoxy and hydroxyl groups from GO which generates pressure leading to the exfoliation GO sheets. This method produces Graphene, which has high structural defects.

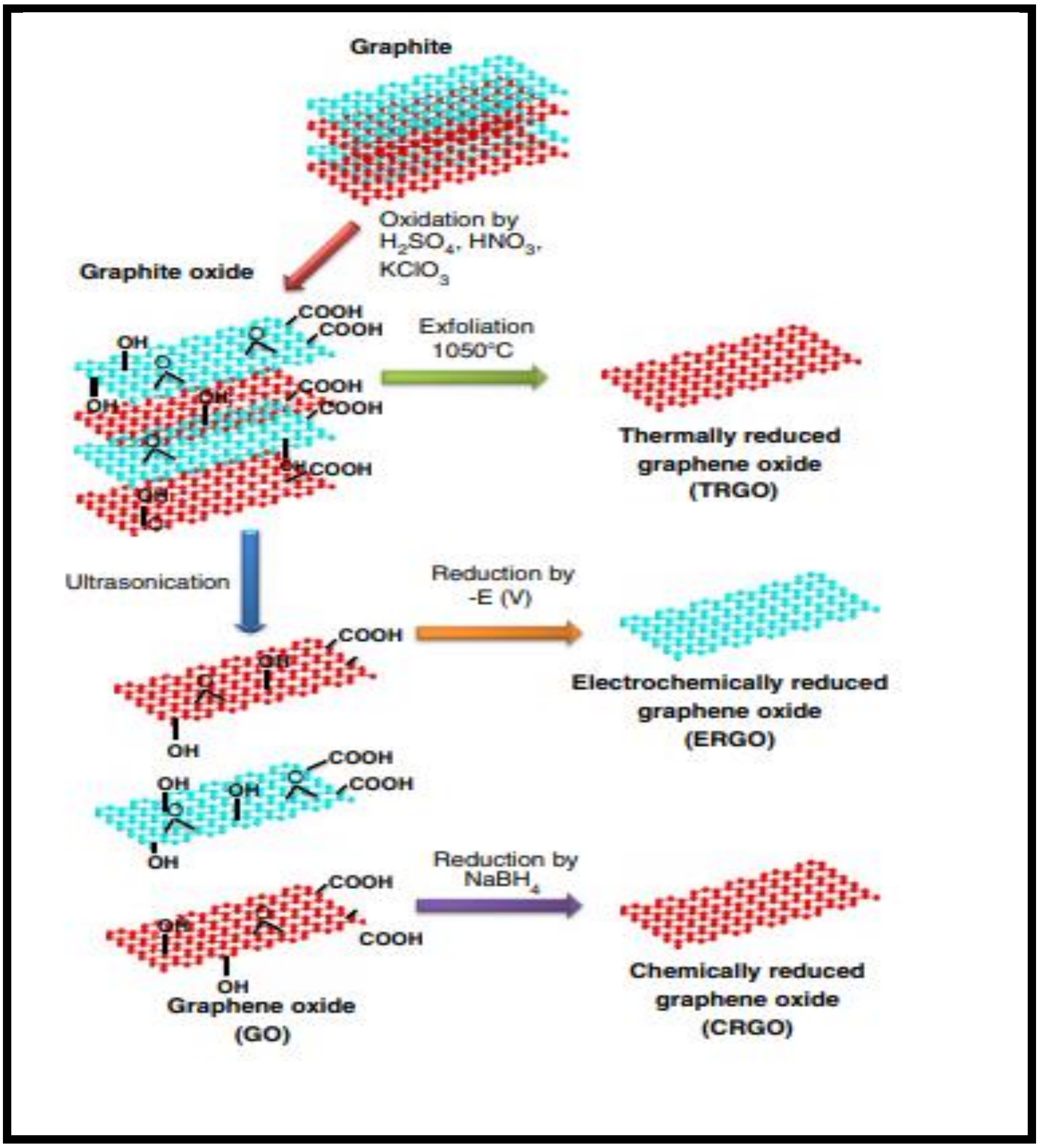

Fig. 3 Schematic Diagram of Synthesis of Graphene by Top down Method

Table 1

Graphene Synthesis by Top Down Method

Method	Thickness	Advantage	Disadvantage
Mechanical Exfoliation	Few layers	Large size and unmodified graphene sheet	Small scale production
Direct sonication of graphite	Single and Multilayers	Unmodified graphene and low cost	Low yield
Electrochemical exfoliation	Single and few layers	Functionalisation and exfoliation with high conductivity	Expensive
Chemical reduction of GO	Single and multiple layer	Large sheet size	Use of hazardous reducing agents
Thermal Reduction of GO	Single and few layer	One step exfoliation and short heating time	High heating temperature and small sheet size of graphene

2.4.2. Bottom up method

This method is very useful for large scale production for the synthesis of graphene. This method is being economical in nature and environment friendly .There are several bottom-up processes such as epitaxial growth on electrically insulating surfaces (SiC), chemical vapour deposition (CVD), unzipping of CNT, arc discharge etc [41]. In CVD method, the carbon atoms is dissolved into a metal catalyst substrate, such as Ni, Cu, Co, Pt, Ir and then precipitate out after cooling, and forming large-scale graphene films [42]. In epitaxial growth process invoved a single crystal SiC substrates which are heated in vacuum at high temperatures and then, the formation of graphene layers by evaporation of silicon atoms from the crystal surface [43].The above two method (CVD and epitaxial growth) are very suitable for synthesis of defect-free uniform graphene sheets for electronic applications. The advantages and disadvantages of bottom up approach are summarized in Table 2 as adopted from Ref. [41].

Table 2

Graphene Synthesis by Bottom up Method

Method	Thickness	Advantage	Disadvantage
CVD	Few layer	Large size, high quality	Small production scale
Arc Discharge	Single layer, bi-layer and few layer	May produce 10g/h of graphene	Low yield of graphene
Epitaxial growth on SiC	Few layers	Large area of graphene	Very small scale production
Unzipping	Multiple layer	Size control	Expensive

2.5. Photoluminescence (PL) of Graphene Based Materials

In this section, we will discussed the PL properties of graphene based material.

2.5.1. Origin of Optical Property of Carbon Based Material

The carbon based materials has both sp^2 and sp^3 bonded regions and the photoluminescence (PL) properties are governed by the π states of the sp^2 cluster [44]. The sp^2domains containing localized π and π* energy levels which reside between the σ and σ* states of the sp3 matrix [45-46]. The PL properties arises due to radiative recombination of electron–hole pairs localized in sp2 domains from such materials [47].Such photoluminescence depends on the fraction of size and shape of sp2 cluster. The electronic band structure of graphene indicates that the valence band (VB) and conduction band (CB) meet each other near the K points (Dirac point).The band gap at the K-points of graphene is zero and thus, graphene does not exhibit PL property.

On the other hand, the VB and CB are well separated in GO. That is the value of DOS is small near the edges of these bands [Fig. 4(b)]. The smaller value of DOS allowed the excited carrier to recombine radiatively by emitting in GO than non radiative recombination of charge carriers. In fact, the PL properties of GO arises from a finite band gap originated due to the presence of both sp2 and sp3 bonded regions [48]. In fact, the origin of PL properties of GO is a controversial issue and discussed in the literature review section.

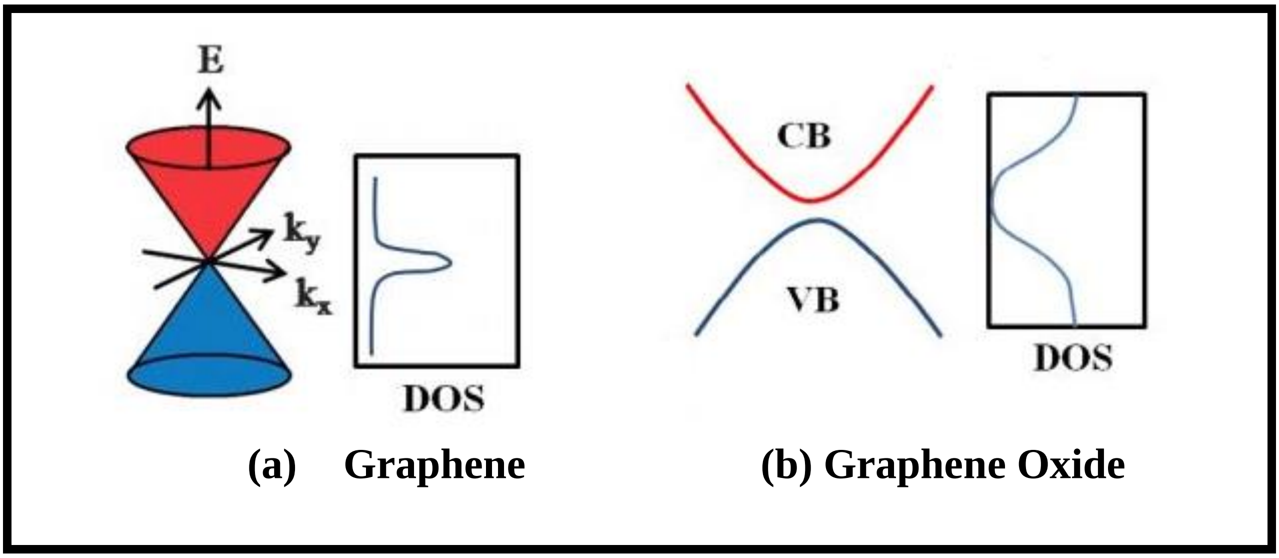

Fig. 4 Electronic Band Structure (a) Graphene (b) Graphene Oxide

2.5.2. Photoluminescence of Graphene

Pure graphene does not normally exhibit PL property due to its zero band gap. However, it exhibits PL property under suitable condition .A few group of researcher reported the PL property of graphene which is originated from both thermalized electron [49-52] and non-thermalized hot electrons [17]. Lui et al. found PL from monolayer pristine graphene which shows emission from the visible to near-ultraviolet region when excited by femtosecond (30 fs) laser pulses [49]. They reported that the fluorescence varies nonlinearly with the excitation fluence and also PL depend on pump fluence which rules out the possibility of hot luminescence due to a two-photon absorption process.The decrease PL with increasing photon energy suggesting that the emission process is thermal in nature. Wang and its co-worker [50] observed nonlinear PL which is broad and very intense in nature from graphene by using the experimental technic femtosecond laser. They compared their observed PL of graphene with the two photon PL spectrum of Au and suggest that PL must be due to the formation of electron hole distribution within 10-20 fs of the excitation by scattering of single photon created carrier. However, the origin of PL from doped graphene due to non-thermalized electrons observed by Chen et al. [53**]**. They explained the PL of doped graphene which is due to the recombination of hot electron and hole. However, due to the zero-band gap of graphene limits its use as an active luminescent material for different optoelectronics and bioimaging applications.

2.5.3. Photoluminescence of Graphene Oxide (GO)

The inability to exhibit PL from graphene is overcome by using chemically functionalised graphene like graphene oxide (GO), reduced graphene oxide (RGO) etc. GO is one of the chemically functionalised form of graphene which exhibits interesting broadband fluorescence properties in the UV, visible and near-infrared spectral regions (NIR) [54-68] and unlike graphene, GO is water soluble which helps to study PL property in aqueous suspension for its optoelectronic applications. Hence, due to its broad band PL property, GO is suitable for material for bio-imaging, sensing and optoelectronics applications like solar cells [69], high luminance light-emitting diodes [70], chemical sensors [71], cellular imaging and drug delivery [72-73], flexible transparent electronics [74]. The observed broad band fluorescence in GO may be explained as the confinement of π electrons in localized sp^2

clusters with different sizes [44, 75-76]. The presence of isolated finite-sized molecular sp^2 clusters which resides within the sp^3 matrix and produces the confinement of π- electrons in GO, resulting in observation of PL by radiative recombination of electron–hole pairs in such sp^2 clusters. The local energy gap depends upon the size of sp^2 clusters which determined [Fig. 5(a)] the wavelength of the emitted PL. The GO structure contains a range of sp^2 cluster sizes, so, the collective band structure has no signature features as depicted in [Fig. 5(b)]. Fig. 5(a) indicates that the PL in the ultraviolet–visible region may occur from sp^2 clusters with sizes of less than 1 nm amounting to ~20 aromatic rings. Red to NIR emission is due to from larger sp2 cluster (>2 nm) possess smaller gaps [76].

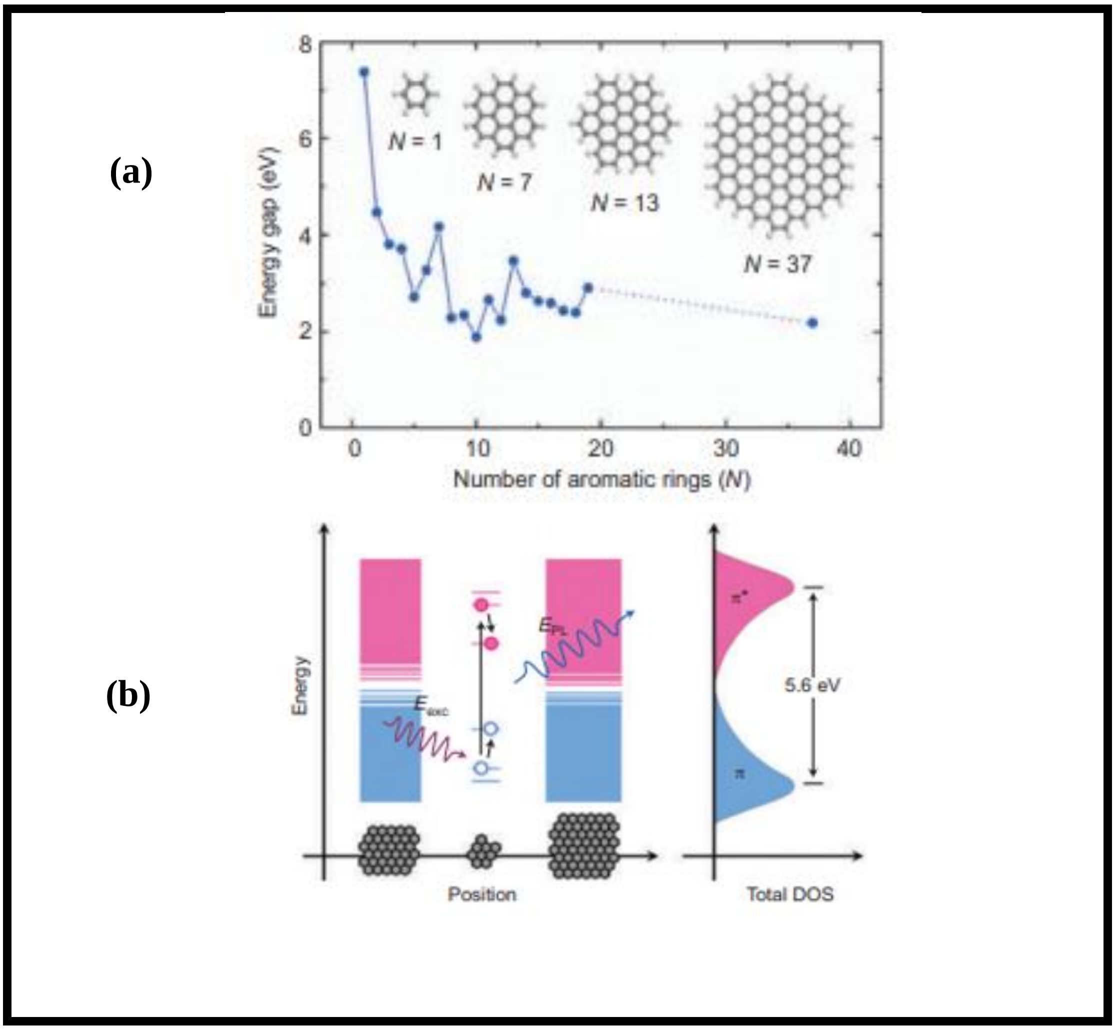

Fig. 5 (a) Calculated energy gap of π–π* transitions as a function of the number of fused aromatic rings (b) Schematic band structure of GO

Luo et al. first time [54] reported the broad photoluminescence (PL) of GO. They observed that both liquid-GO (l-GO) and solid GO (s-GO) exhibits luminescence in the visible and near-IR region and the spectral pattern of PL is more towards the red for s-GO than l-GO. They explained that when the GO flakes in the solution, then the movement of free carriers are confined within the single layer GO but when the GO flakes in solid sample in which strong interlayer interaction creates relaxation roots producing red shifted emission spectral pattern. They also observed that PL is red shifted after the treatment of hydrazine to the GO samples and also found that PL intensity decreases everywhere in the emission spectra with low quantum yield. They explained that non radiative recombination of migrated non equilibrium carriers in the zero band gap region where GO is completely reduced to graphene which decreases the quantum yield. PL properties in the red to NIR region have been observed from laterally nano sized GO aqueous suspensions observed by Sun and co-workers [55]. This kind of similar observation in PL properties also reported by Luo et al [54] from aqueous suspensions and solid samples of the synthesized GO with typical lateral dimensions of 1–10 μm, indicating that the lateral size of the sheets is not the main factor for controlling the emission energy. The broad PL also (red to NIR) reported by Gokus et al. [56] from exfoliated graphene sample after treating an oxygen-plasma through mechanically. The fact that similar PL properties observation from nano sized GO and oxygen-plasma-treated graphene suggesting that the origin of PL is closely related each other. Chhowalla et al. [48] observed blue PL at 390 nm from chemically derived GO thin films deposited from thoroughly exfoliated suspensions and also found that PL peak position shifted about (~ 10 nm) after reduction of GO by using hydrazine vapour. Initially PL intensity increases and then decreases for more exposure to hydrazine vapour i.e. variable PL intensity at 390 nm with the reduction by hydrazine vapour is observed. They also observed red and near IR

(NIR) emission from the chemically derived GO. The evolution of sp2 cluster is shown in [Fig. 6] with the reduction by hydrazine vapour at different time interval.

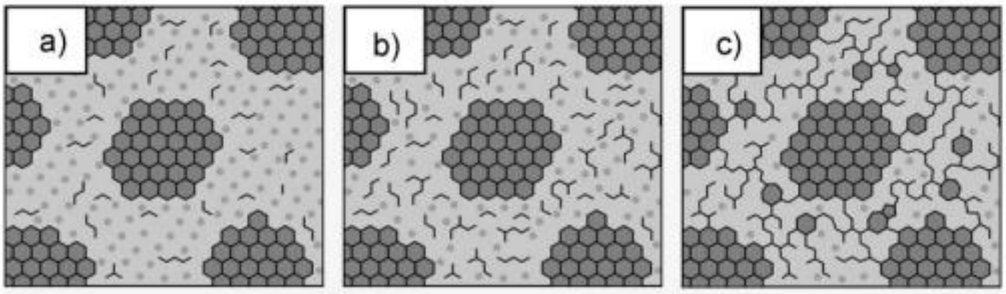

Fig. 6 Model structures of GO (a) as synthesized (b) after moderate reduction and (c) after extensive reduction by exposure to hydrazine vapour

They explained that the origin of blue PL arises from the radiative recombination of electron hole pair within the localized states of smaller sp2 cluster of few aromatic rings. They concluded that the origin of blue PL is markedly different from the origin of emission at visible –NIR [28]. The variable PL intensity is due to the evolution of vary small sp2 clusters. Chen et.al. [57] observed a broad PL from GO samples ranging from 400 to 800 nm and the PL spectra of GO deconvoluted into two Gaussian-like peaks at 600 nm and 470 nm respectively. They also observed that, the PL peaks gradually move towards shorter wavelengths and narrower bandwidths with the progress of reduction under photo thermal reduction. The significant number of disorder-induced defect states within the π-π^* gap in the original GO and shows broad PL spectrum which centered at the longer wavelengths. As a result of deoxygenation, disorder-induced states within the π-π^* gap decreases which increases the number of small sp2 clusters in the reduced GO. The electron hole recombination with small sp2 domain are producing blue luminescence with a narrower bandwidth and diminishing in the emission intensity of the red end emission maxima.

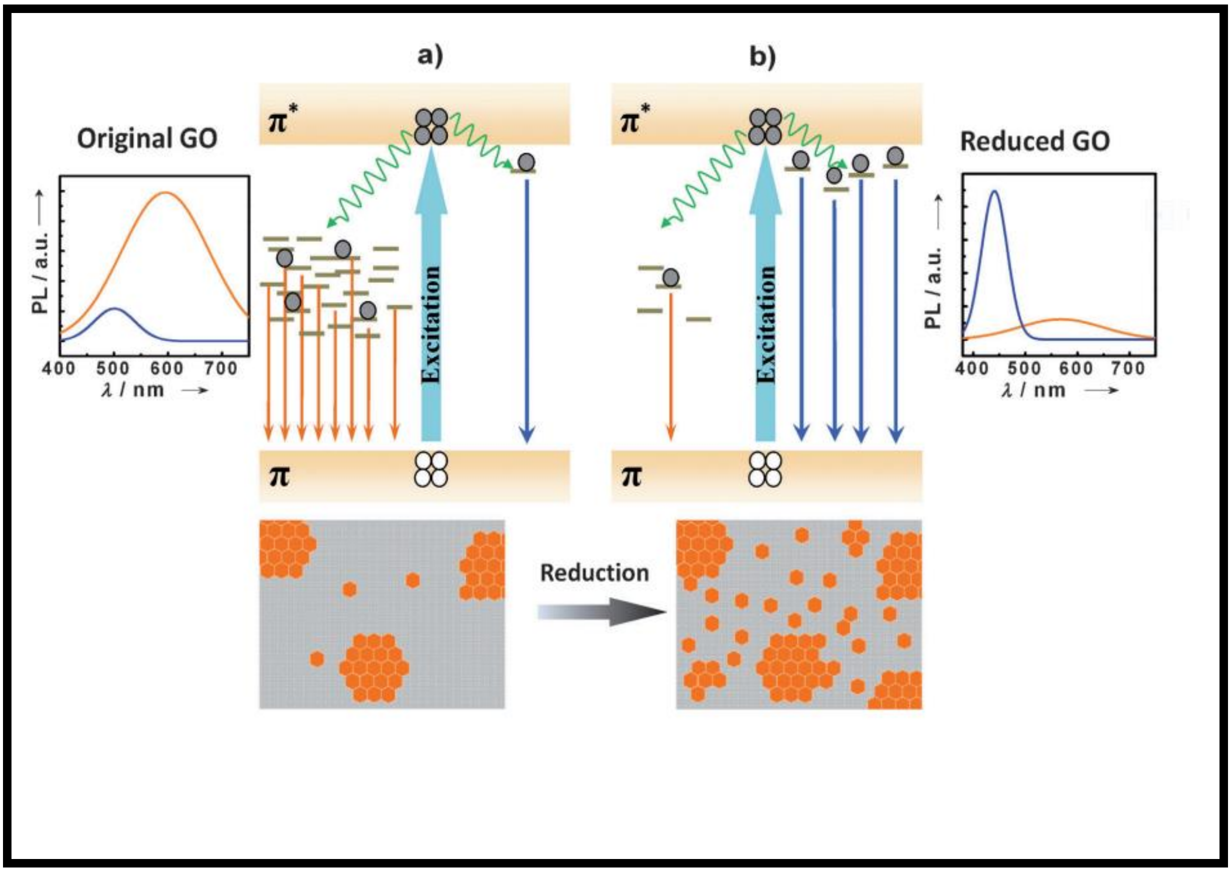

Fig. 7 Proposed PL emission mechanisms (a) the predominant emission at 600 nm from disorder-induced localized states in GO (b) The predominant emission at 470 nm from confined cluster states in RGO

Guo et al. [58] observed no gradual blue shift of emission maxima under hydrothermal reduction of GO to produce reduced GO (R-GO), but this result is explained by the same mechanism [Fig. 7] as proposed by Chien et al. [57]. Xin et al. reported [59] tunable Photoluminescence (PL) of graphene oxide (GO) dispersion from near-ultraviolet to blue region by the controlled reduction under the treatment of hydrazine (N_2H_4).They also found that PL intensity also decreases with the increase of hydrazine concentration. They explained the observed results that it is due to the change in size of smaller sp2 domain by controlled reduction which increases the density of small sp2 nucleus and enhanced the interconnectivity of localized sp2 sites. The quantum yield of PL of GO reported by [48, 54] were very low. The reason for such low yield is non-radiative recombination of excitons in the epoxy and carboxyl groups present in the GO. Blue PL also observed by Dong et al. from GO which is prepared by a bottom–up approach through pyrolyzation of citric acid [60]. They also observed excitation wavelength dependent fluorescence. The PL quantum yield of GO is changed from 2.2% to 3.9% when GO is reduced by $NaBH_4$. However, PL maxima does not change due to reduction. These observations suggest that the removal of oxygen due to chemical reduction which leads to the formation of small sp2 domain having size distribution similar to GO. Therefore, sp2 domains are same for the GO before and after the reduction and hence the PL maxima of GO do not change due to reduction. Mei et al. observed intense blue fluorescence when the GO surface was passivated by amide formation and amination of epoxide with various alkylamines [61]. The alkylamine treated GO shows an emission at 430 nm at the excitation wavelength of 350 nm. They have also found that the PL quantum yield of GO had enhanced by six hundred times (from 0.0002 to 0.13) when GO interact with alkylamines. They have explained that the enhancement of PL is due to the removal of non-radiative recombination sites (epoxy and carboxylic groups) as GO undergoes surface passivation via nucleophilic reactions with alkylamines. Again, It has been found that the several groups has been inspired to study the effect of pH on the fluorescence properties of GO in the aqueous suspension of GO as it contains the functional groups like carboxylic acid and phenoxide groups in the surface and sheet edges respectively [62-65] Galande et al. reported the strongly pH-dependent broad band visible fluorescence from aqueous dispersion [62]. They observed unchanged spectral pattern with the decrease in intensity of the emission peak when pH increased from highly acidic (pH -1.6) towards neutral values [Fig. 8].

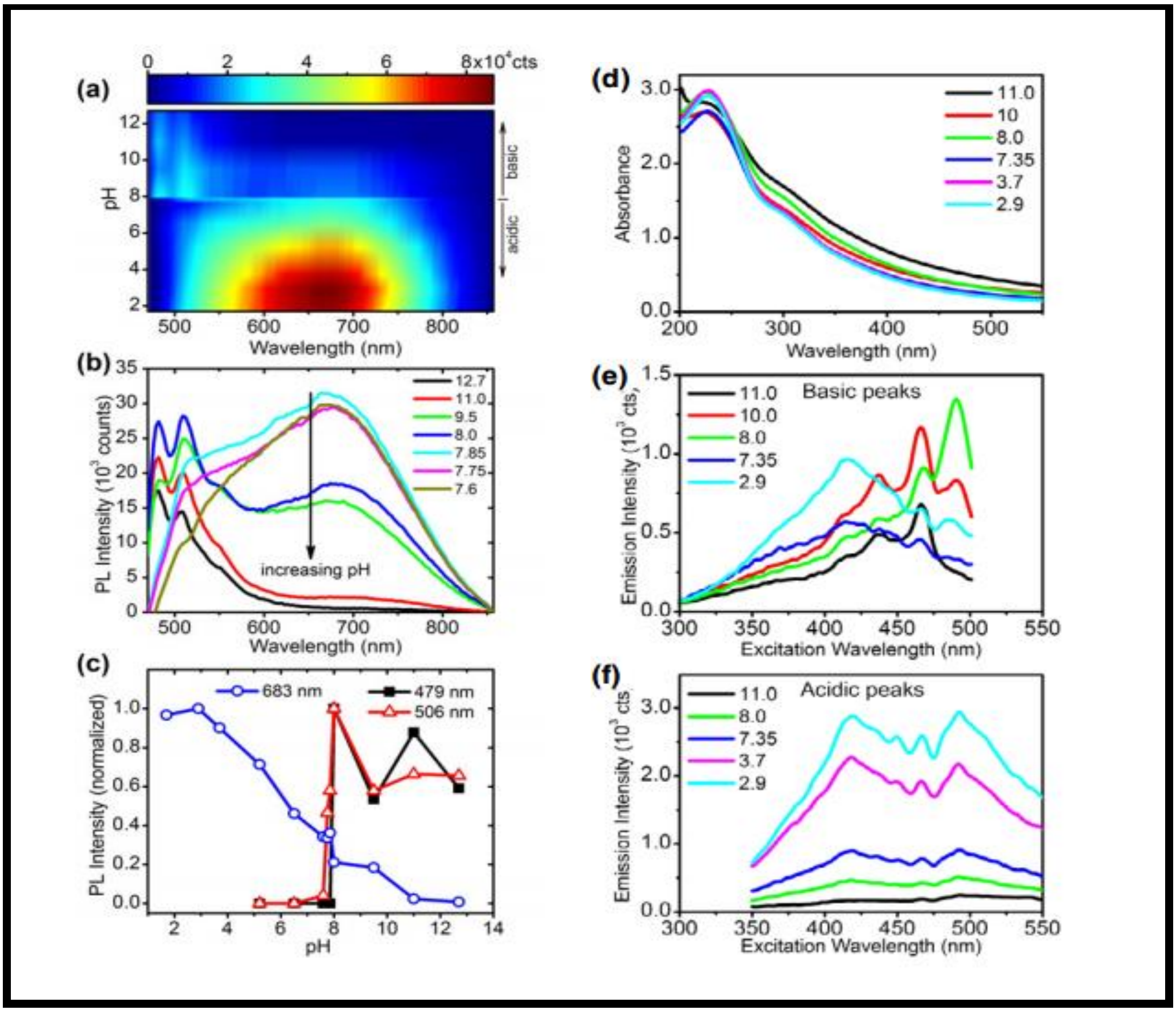

(a) Pl spectra for sample of pH values between 1.7 and 12.7 (λex~ 440 nm)

(b) Pl spectra for pH in the basic range from 7.6 to 12.7 (λex~ 440 nm),

(c) Intensity variation of PL peaks (479, 506 and 683 nm) with the pH

(d) Absorbance spectra of GO measured at pH values between 2.9 and 11.

(e) Excitation spectra measured for emission at 511 nm

(f) Excitation Spectra measured at 665 nm for pH ranges between 2.9 and 11

Interestingly, when the pH is above 7, they observed disappearance of the peak at 668 nm and formation of two new peak at 482 nm and 506 nm respectively. The observed result is completely reversible in nature within measured pH range and suggested that no change in oxygen containing species. They explained that the emission feature above pH = 8 is due to from the excited state G-COO$^-$ and below pH =8 from G-COOH* which are formed from the excited state protonation of the G-COO$^-$. The G-COO$^-$ species are responsible for the red shifted emission. In fact the fluorescence of GO originated from quasi-molecular fluorophore (containing 50 π-electron and carboxylic acid groups) similar to polycyclic aromatic compounds. By using time resolved spectroscopic technique, the first time reported the dual emission feature from GO at 400 nm (blue band) and 740 nm (long wavelength) coexistent by Zhang et. al. [63]. They also found that the intensity of the peaks and the emission maxima are strongly dependent on the concentration GO, pH of the medium and the excitation energy. The emission band becomes broader and red shifted gradually as the concentration of the GO was increased. The blue emission band was favourable at low GO concentration due to self-adsorption to its fluorescence is very low. The band shape becomes distorted as the concentration of GO is increased due self-reabsorption of emitted radiation is very high and the distortion is more affected at the blue or UV region. The long wavelength band is major al very low pH whereas blue band is appeared as major at high pH values. This result suggesting that long wavelength band is originated from the protonated GO and blue band is arises from the GO only.

Fig. 9

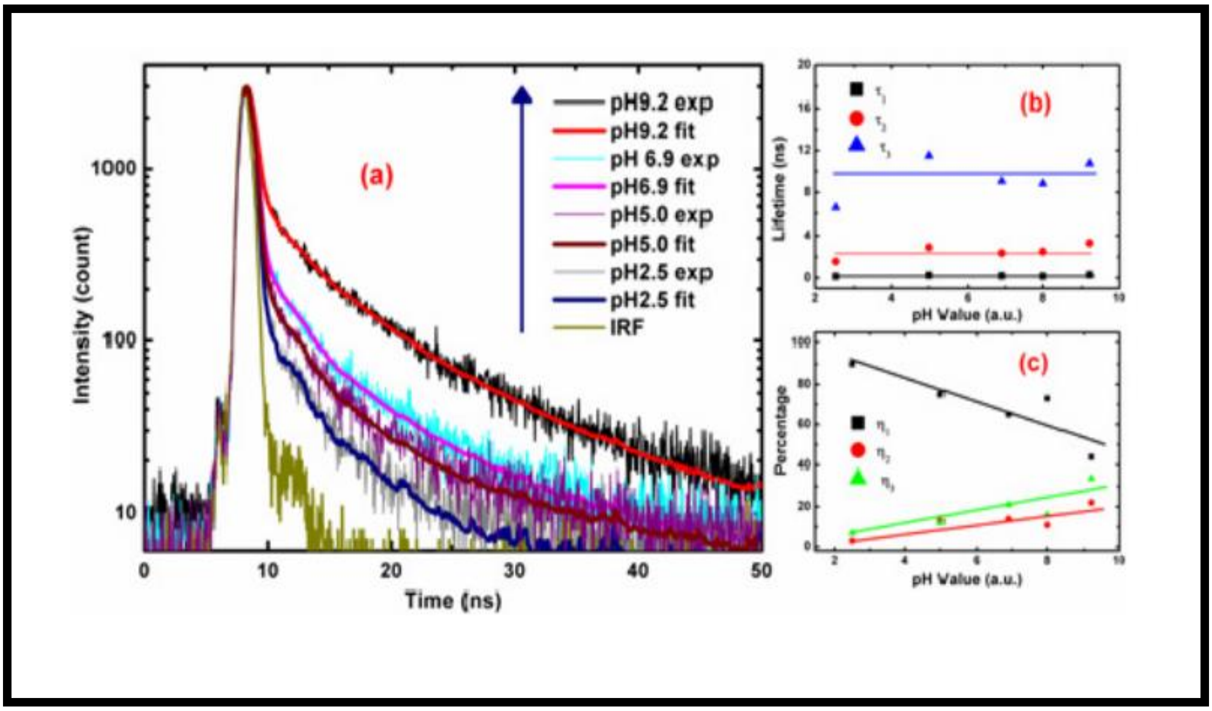

(a) The PL decay Measured at 470 nm in different pH (λ_{ex}~ 379 nm)

(b) The dependence of the fluorescence lifetime components on pH

(c) The dependence of percentage contribution to total emission on pH

Matsuda et al. [64] first time observed ultraviolet (UV) fluorescence at 300 nm (P_1) in addition to blue fluorescence 440 nm (P_2) [48,57,63] from the aqueous dispersion of highly exfoliated GO [Fig. 9 and Fig. 10]. They have found that the PL excitation (PLE) spectra corresponding to both the emission bands do not identical with the absorption spectra and suggesting that different absorbing and emitting species existent within GO. They also observed that the emission band also pH dependent. They suggest that the photoluminescence originates from sp2 cluster consisting of few number of aromatic ring with oxygen containing functional group acting as PL centers in the GO.

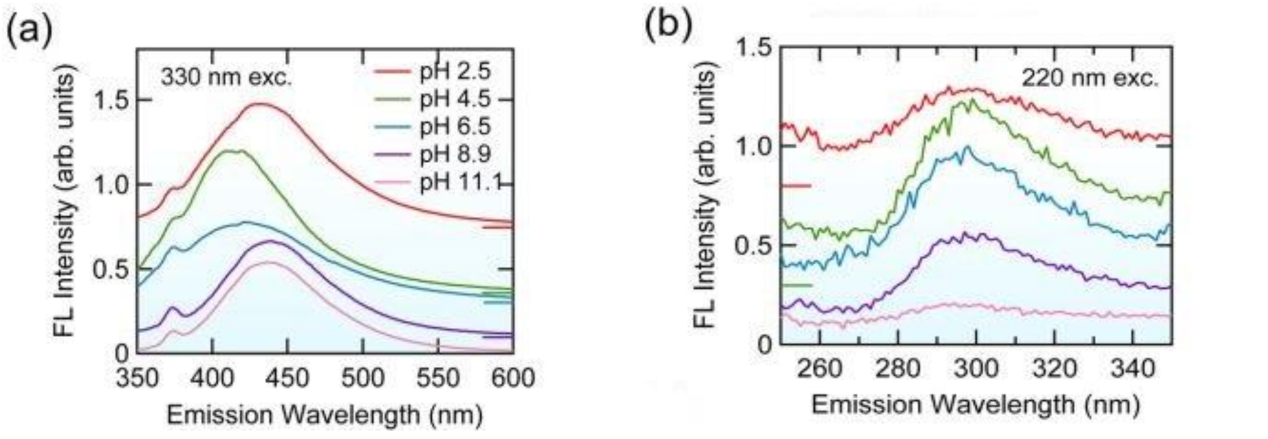

Fig. 10 PL spectra GOs at different pH (a) Ex. Wl. 330 (b)Ex. Wl. 220 220 nm

Bharathi et al. [65] observed pH dependent emission feature in the visible region from aqueous dispersion of GO which consists of quasi-molecular functional group. They suggested from time resolved emission spectra of GO that both type of intermolecular and intramolecular excited state proton transfer (ESPT) is occurred involving spectral migration from 407 nm to 430 nm. They concluded that the observed emission feature (ESPT) almost similar to that exhibited by 3-hydroxy napthoic acid which is shown in the schematic diagram [Fig. 11]. Dutta et al. reported the blue shift of UV fluorescence from aqueous dispersion of GO with the increase in pH. When they excited at 240 nm and 280 nm, they observed 32 nm blue shift and 12 nm blue shift respectively with the increase in pH [Fig. 12], because of the movement of basal planes of GO by the repulsion of carboxylate ions of GO sheets , which weakening the π-π stacking interaction [66].

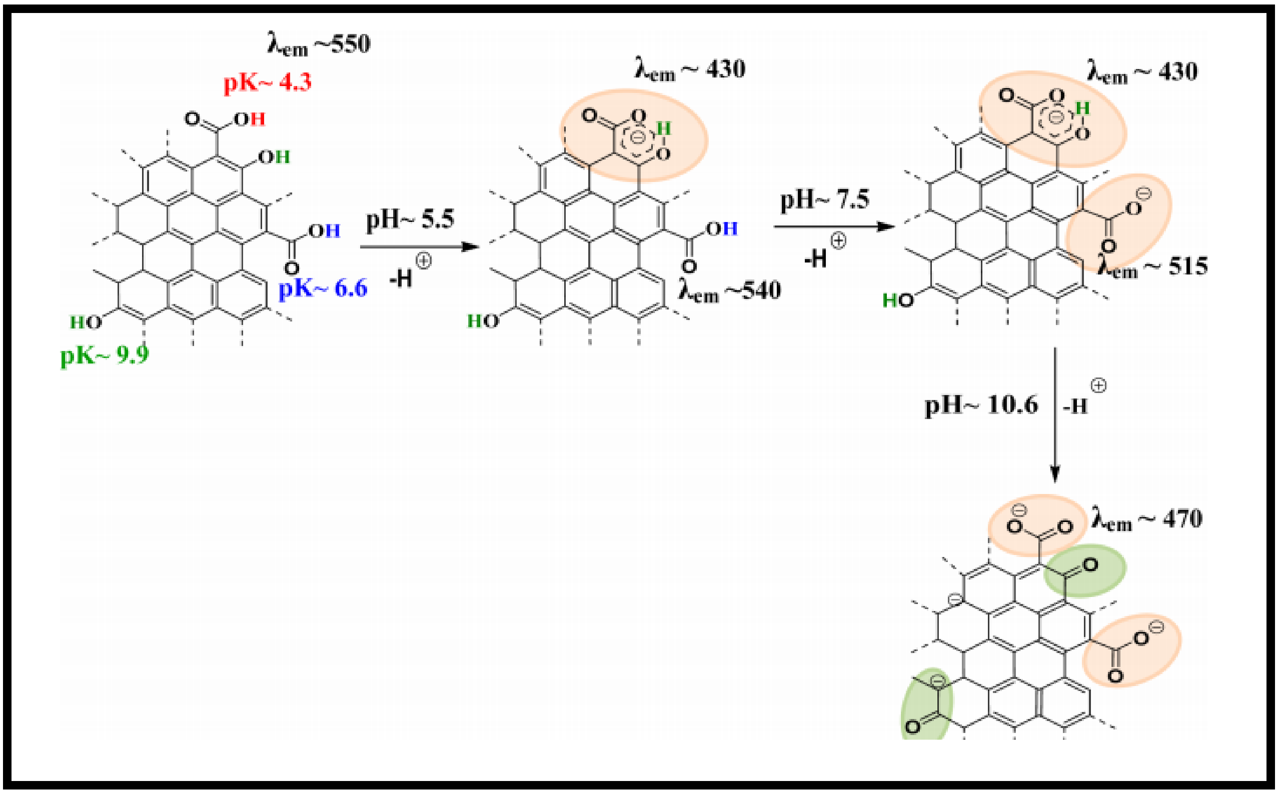

Fig. 11 Schematic Diagram of Proton Transfer from GO

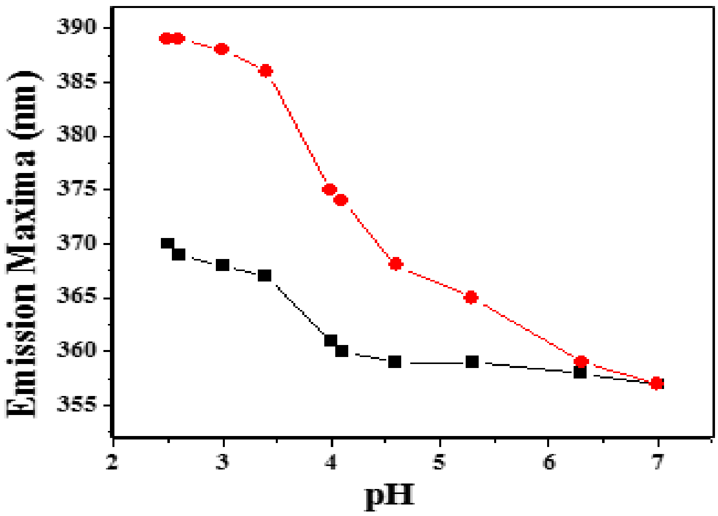

Fig. 12 Plot of Emission maxima (nm) vs pH λ_{ex} = 280 nm (■), λ_{ex} = 240 nm (●)

Shang et al. reported multi exponential decay kinetics ranging from 1 ps to 2 ns of graphene oxide in water by using time-resolved fluorescence measurements. They suggested that the origin of the fluorescence because of the electron-hole recombination from the bottom of the conduction band and wide-range valance band of localized states [67]. Kikkawa et al. [68] investigated the photoluminescence feature in graphene oxide and reduced graphene oxide by using sub picosecond time-resolved emission measurements. They reported broad photoluminescence spectra from both graphene oxide and reduced graphene oxide. They observed progressive red shift of the emission spectrum as substantial energy redistribution and relaxation among the luminating states within the first few picoseconds. Under photothermal reduction at different time interval of GO, blue shifts of PL is observed which is similar to the observation of Ref-56. It is also reported the origin of strong excitation wavelength dependent emission feature of GO by Cushing et al. [77]. They explained that the origin of excitation wavelength in GO is due to “giant red-edge effect”. When GO present in polar solvent, the solvation dynamics slows down to the same time scale as the fluorescence because of the local environment of the GO sheet, resulting in broaden in spectra with red shift up to 200 nm. This effect is disappeared in nonpolar solvent, i.e. independent of the excitation wavelength and narrow fluorescence peak is observed in nonpolar solvent. [Fig. 13].

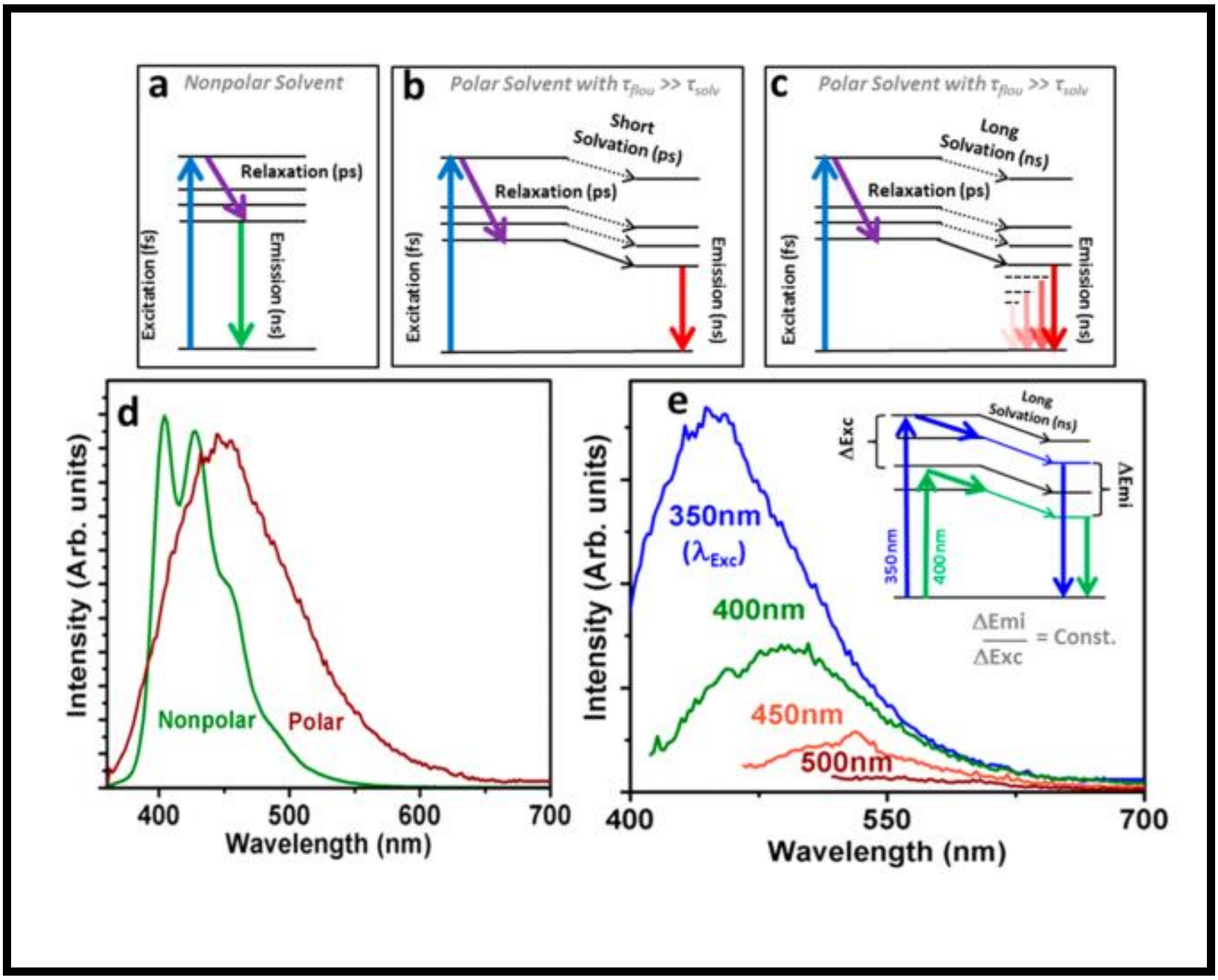

Fig. 13 (a) Fluorescence in a nonpolar solvent (b) Fluorescence in a polar solvent. (c) If the solvent interactions are on the same time scale as the fluorescence lifetime, a time-dependent emission is created, resulting in a red-edge tail. (d) In a nonpolar solvent (pentane), fluorescence of GO is independent of excitation wavelength and red-shifts the emission maxima in a polar solvent (water) (e) The relaxation of the time-dependent emission energy is independent of excitation wavelength.

They also explained the fluorescence mechanism of graphene oxide (GO). They reported that an excited state protonation observed from the COOH group of GO and the excitation wavelength dependent fluorescence is due to the presence of polar groups such as the OH moiety in the GO sheets. The fingerprinting'' photoluminescence feature from GO involving three peak is observed by Nianqiang et al. [78]. They explained that the three peak originated from $\sigma*$ to n, $\pi*$ to π and $\pi*$ to n electronic transition. The following functional group C–OH, the aromatic C=C and the C=O are associated with the observed three PL peaks. They reported that the relative PL intensities of the peaks can be modulated by changing the oxygen-containing functional groups. Helen et al. [79] treated the GO with sodium hydroxide (NaOH), GO material separated into two part. They observed that one is highly fluorescent (high intensity), colourless oxidative debris and another is non-fluorescent material of darker graphene like sheets. They found that PL intensity of oxidative debris is more than their produced GO and also blue shifting in PL of the oxidative debris is observed [79]. Ozcan et al. [80] reported the effect of functional group and associative behaviour of GO on the fluorescence of graphene oxide. According to them, fluorescence consists of six components and the relative intensity of the six component changes significantly due to reduction. The hydrogen bond suppress the emission from smaller sp2 domain, while the large domain remain almost unaffected due to reduction [80]. Shao et al. observed fluorescence from chemically derived graphene (CDG). They also studied the effect of self-rolling up and aggregation on the PL properties of CDG [81]. Again, it has been found that the band gap of GO depends upon the method of synthesis. To date, different methods of GO synthesis has been developed including Hummers/modified Hummers methods [13, 82], the reaction between benzoyl peroxide and graphite [83], oxygen plasma treated mechanical exfoliation [56], the different chemical synthesis [48, 84-88], and other structure-defining synthetic methods [89-84]. Depending on the method of synthesis procedures, the ratio of carbon atom to oxygen atom of GO changes [89-92, 95-100] and therefore, the distributions of different functional group which leads to the modification of optical and electronic properties of GO. For example, GO synthesized via chemical reaction shows ultra-violet/blue emission [84-85], GO and graphene oxide quantum dots synthesised by top-down approach exhibits green fluorescence [94-95], oxygen plasma treated GO/nano graphene oxide displays red/near-infrared photoluminescence [55-56]. In addition, GO emission intensity also varies [96-97] depending on the degree of functionalization and the production method. These variations in electronic and optical configurations allow GO for multiple potential applications in optoelectronics [98-99] or sensing [100].

2.5.4. PL of Graphene Quantum Dot (GQD)

In the earlier section of PL of GO, it has been discussed the origin of the PL property of GO which is necessary to understand the PL of GQD, because GO is an important raw material for GQD synthesis. Therefore, GO and GQDs possess similar chemical structures. GQD has more defects and possess oxygen groups, and functional groups on the surface as like GO. It is well reported that GO exhibits PL in wide range in the electromagnetic spectrum and thus, the PL results obtained from GO will be used to understand the PL of GQD. It has been observed that excitons in graphene have an infinite Bohr diameter. Thus, quantum confinement effects has been observed from any size of graphene fragments and so it will open a non -zero band gap for GQD and produces PL on excitation. This band gap is depend on the the size and surface chemistry of the GQD [101]. So, it has been tremendous attention for researcher to develop GQDs and a group of researcher reported a reasonable PL mechanisms for GQD. Alam et al. theoretically investigated the PL mechanism of GQD [102]. By using density functional theory and time-dependent density calculations, they studied the PL properties of GQD systematically. The results indicated that the PL of zigzag-edged GQDs may cover the entire visible light spectrum by changing the diameter from 0.89

to 1.80 nm. The chemical functionalities and defects may induce a red-shifted PL whereas Armchair edges and pyrrolic N-doping can cause a blue-shift. Single layered nano-sized (< 10 nm) graphene oxide (NGO) produces PL in the visible, IR and NIR regions in 2008 reported by Sun et al. [55,103]. Surprisingly, due to size reduction, they did not observe any quantum confinement effect. They explained the observed fact by proposing that each NGO sheet has conjugated domains which has different sizes equal to small aromatic molecules to large macromolecular domains. Blue Pl obtained from GQDs of average diameter 9.6 nm (having 1-3 layers), reported by Wu et al. [104]. They observed excitation wavelength dependent PL from GQD, which shifts towards red as excitation changes from 320 to 420 nm. They also reported that the PL is pH dependent. In addition to the blue PL, excitation wavelength dependent green fluorescence has been obtained from smaller size GQDs [105-106]. It has been also reported that the HOMO–LUMO energy gap depends on the size of the graphene fragments [107]. As the diameter of GQDs decreases, the energy gap increases gradually and as a result excitation dependent emission is reported for mixtures of different particle size GQDs. So, the PL property of GQDs may be considered to be originated as a result of LUMO to HOMO transitions. Hong and co-workers [108], observed that the PL energy decreases with the increase of size of GQD up to a limit (~ 17 nm) holding quantum confinement effect. But, the increasing size of GQD for bigger particles, PL energy increases. They explained this anomalous behaviour due to the transformation of the shape. The PL of GQD may be developed via surface passivation. Shen et al. [109] reported that GQD passivated by polyethylene glycol (PEG) which produces a excellent PL properties, and higher fluorescence quantum yield for the blue emission band. They also observed pH dependent PL intensity. GQD produces intense PL at neutral pH, which higher from the medium of both acidic and alkaline environments. It is also reported that PL performance may also be affected by the solvent. Pal and co-workers [110] observed blue PL from GQDs and also they measured PL decay which was found to be bi-exponential in nature with a fast and a slow lifetime components. Similar PL decay profiles reported by Kim et al. [111] and they explained that the longer one for size-dependent slow transition as a result of the edge-state variation and the shorter lifetime for size-independent band-to-band transition of GQDs.

2.5.5. Application of PL of Chemically Derived Graphene

Chemically derived graphene shows PL over a wide range from UV to NIR in the electromagnetic spectrum and the researcher uses the PL properties of chemically derived graphene in different field. Liu et. al. the resulting Poly-ethylene glylated -NGO exhibited excellent stability in all biological solutions and used PL from this material for delivery of water insoluble cancer drug. They detected B-cells successfully by monitoring the quenching of the strong NIR fluorescence [112]. Yu et al. has been synthesised a peptide-linked polymer dots which has assembled with graphene oxide surface. Hence, they produced a nano complex (graphene oxide-peptide-polymer dot) and used it for sensitive, rapid, and accurate detection of matrix metallo proteinase-9 by measuring the fluorescence [113].Chen et al. developed a stable and covalent linked fluorescein isothiocyanate-labeled peptide with reduced nano graphene oxide (nrGO-Pep-FITC) and this developed nano material has been used as fluorescent probe for ultrasensitive detection of matrix metalloproteinase-9 (MMP-9) [114]. Dinda et al. have synthesised 2,6-diamino pyridine functionalized graphene oxide material (DAP-RGO)which produces a bright luminescent and they used for selective detection of TNP in the presence of other nitro compounds [115]. Gong and co-workers [116] observed up-conversion fluorescence from N-GQDs and used for deep tissue and cellular imaging. The material like GQD produces a strong PL which has been used as a fluorescence sensor to detect many analytics. The PL of GQDs is quenched by Fe^{3+} ion observed by Jin et al. in 2012 [117] due to charge transfer interaction and they used for selective detection of ferric ions. Chi et al. detected free chlorine in drinking water by observing change of the PL property of GQDs [118]. Under physiological condition using GQDs, Pal and co-workers [110] reported the fluorescence chemo sensing of Hg2+ in aqueous medium. Fan et al. efficiently detected tri nitro toluene (TNT) from fluorescence turn-off of GQDs [119]. The detection of Cu2+ ion was reported by Sun et al. using a fluorescence probe of amino-functionalized GQDs [120]. Photoluminescence turn-off mechanism of GQDs was also used for bio-sensing. Zhao et al. [121] observed PL quenching of GQD functionalized by mouse antihuman immunoglobulin G antibody (mIgG) in the presence of graphene and used this material for the detection of human immunoglobulin (IgG). Ran et al. [122] proposed efficient and selective pathway for sensing of thiols using GQDs which was decorated by silver and then metal clusters interact with defect sites of GQD and thereby PL quenching observed which helped to detect thiols group. PL turn-on mechanism was applied for the sensitive detection of phosphate [123] and glucose [124]. Liu et al. [125] reported that the PL of glutathione functionalized GQD turned-off in the presence of Fe2+. Saha et al. synthesised graphene oxide which is functionalized by thymine and utilised the material for detection of both Hg^{2+} and I^{-} ion selectively using fluorescence turn-off-on mechanism [126]. Again, in the presence of phosphate containing molecule, the PL turned-on and they was used this PL for the determination of the ATP level in cell lysates and human blood serum successfully. The high quantum yield of the PL and tunability of the PL of GQD material helps to use in organic light emitting diodes (OLEDs) [127]. Tang et al. [127] observed the appearance of a red shifted broad band emission from GQD and they used GQDs in commercially available blue-light-emitting diodes. Son et al. [129] improved the efficiency of white-light-emitting LEDs by coating ZnO nanoparticles with GQDs and observed a brightness of 798 cd m−2. By using GQD–agar composite in commercial blue-light-emitting diode, Lau and co-workers [130] reported a white-light-emitting diode.

2.6. Reference

[1] K. S. Novoselov, A. K. Geim, S. V. Morozov, D. Jiang, Y. Zhang, S. V. Dubonos, I. V. Grigorieva and A. A. Firsov, *Science*, 2004, **306**, 666-669.

[2] K. S. Novoselov, A. K. Geim, S. V. Morozov, D. Jiang, M. I. Katsnelson, I. V. Grigorieva, S. V. Dubonos , A. A. Firsov, *Nature*, 2005, **438**, 197-200.

[3] C. N. R. Rao, A. K. Sood, K. S. Subrahmanyam and A. Govindaraj, *Angew Chem. Int. Ed*., 2009, **48**, 7752-7777.

[4] X. Dong, L. Wang, D. Wang, C. Li and J. Jin, *Langmuir*, 2012, **28**, 293–298.

[5] L. Qu, Y.Liu, J. B. Baek and L. Dai, *ACS Nano*, 2010 **4(3)** 2–1326.

[6] X. Wang, L. J. Zhi, N. Z. Tsao, J. L. Li. Tomovic and K. Mullen, *Angew. Chem. Int. Ed*., 2008, **47**, 2990–2292.

[7] S. Zhang, K. Yang, L. Feng and Z. Liu, *Carbon*, 2011, **49**, 4040–4049.

[8] B.C. Brodie, On the Atomic Weight of Graphite. Philosophical Transactions of the Royal Society of London 1859,**149**, 249-59.

[9] V. Kohlschütter, P. Haenni, Z. Kenntnis *Zeitschrift für anorganische und allgemeine Chemie* 1919, **105(1),** 121-44.

[10] J. D. Bernal, The Structure of Graphite. Proceedings of the Royal Society of London Series A, Containing Papers of a Mathematical and Physical Character 1924,106 (740),749-73.

[11] P. R Wallace, *Physical Review* 1947, **71 (9)**, 622-634.

[12] G Ruess, F. Vogt, Monatshefte für Chemie 1948, **78(3-4)**, 222-42.

[13] W.S. Hummers, R.E. Offeman, *J Am Chem Soc* 1958, **80(6)**, 1339

[14] H.P. Boehm, A. Clauss, G.O. Fischer, U. Hofmann, *Zeitschrift für anorganische und allgemeine Chemie* 1962, **316(3-4)**, 119-27.

[15] S. Mouras, A. Hamm D. Djurado J.C. Cousseins, *Revue de Chimie Minerale* 1987, **24**, 572-582.

[16] T. Ohta, A. Bostwick, T. Seyller, K. Horn, E. Rotenberg, *Science*, 2006, **313(5789),** 951-4.

[17] W. Cai, R.D. Piner, F.J. Stadermann, S. Park, M.A. Shaibat, Y. Ishii, D. A. Velamakanni, S.J. An, M. Stoller, J. An, D. Chen, R.S. Ruoff, *Science*, 2008, **321(5897**), 1815.

[18] D. Yang, A. Velamakanni, G. Bozoklu, S. Park, M. Stoller, R.D. Piner, *Carbon*, 2009, **47(1)**, 145-152.

[19] A.K. Geim , K.S. Novoselov, *Nature Mater*, 2007, **6**, 183–191.

[20] K.S. Novoselov , V. Falko , L.Colombo, P.R. Gellert, M.G. Schwab , K. Kim, *Nature*, 2012, **490**, 192-200.

[21] M. H. Kang, L. O. P. López, B. Chen, K. Teo, J. A. Williams, W. I. Milne, M. T. Cole, *ACS Appl. Mater. Interfaces*, 2016, **8**, 22506- 22515.

[22] A.K. Geim, *Science*, 2009, **324**,.1530-1534.

[23] J.C. Meyer, A. K. Geim, M. I. Katsnelson, K.S. Novoselov, T.J. Booth, S. Roth, *Nature*, 2007,**446**, 60–63.

[24] J. C. Slonczewski , P. R. Weiss, *Phys. Rev*, 1958, **109**, 272-279.

[25] A. Bostwick , T. Ohta , J. L. McChesney , K.V. Emtsev , F. Speck , T.Seyller , K. Horn , S.D. Kevan , E. Rotenberg, *New Journal of Physics*, 2010, **12**, 125014.

[26] A.B. Kuzmenko, E.Van Heumen, F. Carbone, *Phys. Rev. Lett*, 2008, **100**, 117401.

[27] R.R. Nair, P. Blake, A.N. Grigorenko, K.S. Novoselov, T.J. Booth, T.Stauber, N.M.R. Peres, A.K. Geim, *Science*, 2008, **320**, 1308.

[28] Z.Q. Li, E.A. Henriksen, Z. Jiang, Z. Hao, M.C. Martin, P. Kim, H.L. Stormer, D.N. Basov, *Nat. Phys*, 2008, **4**, 532–535.

[29] K.S. Novoselov, Z. Jiang, Y. Zhang, S.V. Morozov, H.L. Stormer, U. Zeitler, J.C. Maan, G.S. Boebinger, P. Kim, A.K. Geim, *Science,* 2007, **315**, 1379-1379.

[30] M. Coroş, F. Pogăcean, M. C. Roşu, C. Socaci, G. Borodi, L. Mageruşan, A. R. Birişa and S. Pruneanu, *RSC Adv.,* 2016, **6**, 2651- 2661.

[31] M. Yi and Z. Shen, *J. Mater. Chem. A*, 2015, **3**, 11700-11715.

[32] H. Zhang, J. Ye, Y. Ye, Y. Chen, C. He and Y. Chen, *Electrochim. Acta.,* 2014, **138**, 311-317.

[33] H. V. Kumar, S. J. Woltornist, D. H. Adamson, *Carbon,* 2016, **98**, 491-495.

[34] D. R. Dreyer, S. Park, C. W. Bielawski and R. S. Ruoff, *Chem. Soc. Rev.,* 2010, **39**, 228-240

[35] D.K. Gupta, R. S. Rajaura, K. Sharma, *International Journal of Environment on Science and Technology*, 2015, **1(1),** 16-24

[36] J. Zhao, L. Liu, F. Li, Springer Heidelberg, NewYork, 2015

[37] Y. Zhu , S. Murali , W. Cai , X. Li, J. Suk , J. R. Potts , R. S. Ruoff, *Adv. Mater.* 2010, **22,** 3906–3924.

[38] R. J. seresht, M. Jahanshahi, A.M.Rashidi, A. A.Ghoreyshi, *Iranica Journal of Energy & Environment*, 2013, Special Issue on Nanotechnology, 53-59,

[39] U. S. Poornima and Y. Narayana, *International Journal of Advanced Scientific and Technical Research,* 2015, **5(5),** 1-12

[40] M.J. McAllister, J.L. Li, D.H. Adamson, H. C. Schniepp, A. A. Abdala, J.Liu, M.H. Alonso, D. L. Milius, R. Car, R. K. Prud'hommeI.A. Aksay, *Chem. Mater*., 2007, **19**, 4396-4404.

[41] H. Kim, A. A. Abdala, C. W. Macosko, *Macromolecules*, 2010, **43**, 6515-6530.

[42] X. Wang, H. You, F. Liu , M. Li, L.Wan, S. Li,, Q. Li, Y. Xu, R. Tian, Z. Yu, D. Xiang, J.Cheng, *J.Chem.Vap. Deposition*, 2009, **15**, 53-56.

[43] E. Rollings, G.H. Gweon, S.Y. Zhou, B.S. Mun, J.L. McChesney, B.S. Hussain, A.V. Fedorov, P.N. First, W.A. Heer, A. Lanzara, J. Phys. Chem. Solids, 2006, **67**, 2172-2177.

[44] J. Robertson, E.P. O'Reilly, *Phys Rev B*, 1987, **35(6),** 2946-57.

[45] C Mathioudakis, G Kopidakis, P.C. Kelires, P. Patsalas, M. Gioti, S. Logothetidis, *Thin Solid Films* 2005, **482(1-2**), 151-5.

[46] C.W. Chen, J. Robertson, *J Non-Cryst Solids*, 1998, **227**, 602-6.

[47] T. Heitz, C. Godet, J.E. Bouree, B. Drevillon, J.P. Conde., *Phys Rev B*, 1999, **60(8)**, 6045-52.

[48] G. Eda, Y. Y. Lin, C. Mattevi, H. Yamaguchi, H. A. Chen, I. S. Chen, C. W. Chen, M. Chhowalla, *Adv. Mater.*, 2010, **22**, 505-509.

[49] C.H. Lui, K.F. Mak, J. Shan, T.F. Heinz, *Phys Rev Lett*, 2005, **105(12),** 127404.

[50] W.T. Liu, S.W. Wu, P.J. Schuck, M, Salmeron, Y.R. Shen, F. Wang. *Phys Rev B*, 2010, **82(8)**, 81408

[51] S. Berciaud, M.Y. Han, K.F. Mak, L.E. Brus, P. Kim, T.F. Heinz, *Phys Rev Lett*., 2010, **104(22),** 227401.

[52] M. Freitag, H.Y. Chiu, M. Steiner, V. Perebeinos, P. Avouris, *Nat Nano*, 2010, **5(7)**,497-501.

[53] C.F. Chen, C.H. Park, B.W. Boudouris, J. Horng, B. Geng, C. Girit, A. Zettl, M.F. Crommie, R.A. Segalman, S.G. Louie, F. Wang, Nature, 2011, **471(7340)**, 617-20.

[54]Z. Luo, P. M. Vora, E. J. Mele, A. T. C. Johnson, J. M. Kikkawa, *App. Phys. Lett.*, 2009, **94**, 111909-1-3.

[55] X. Sun, Z. Liu, K. Welsher J.T. Robinson, A. Goodwin S. Zaric. *Nano Res.*, 2008, **1(3)**, 203-12

[56] T. Gokus, R. R. Nair, A. Bonetti, M. Böhmler, A. Lombardo, K. S. Novoselov, A. K. Geim, A. C. Ferrari, A. Hartschuh, *ACS Nano*, 2009, **3**, 3963–3968.

[57] C. T. Chien, S. S. Li, W. J. Lai, Y. C. Yeh, H. A. Chen, I. S. Chen, L. C. Chen, K. H. Chen, T. Nemoto, S. Isoda, M. Chen, T. Fujita, G. Eda, H. Yamaguchi, M. Chhowalla, C. W. Chen, *Angew Chem. Int. Ed*., 2012, **51**, 6662-6666.

[58]C.H.Chuang,Y.F.Wang,Y.C. Shao, Y.C.Yeh, D.Y. Wang, C.W.Chen, J. W.Chiou,Sekhar C. Ray, W. F. Pong, L. Zhang, J. F. Zhu & J. H. Guo, *Scientific Reports*, 2014, **4**, 4525.

[59] G. Xin , Y. Meng , Y. Ma , D. Ho , N. Kim , S. M. Cho , H. Chae., *Materials Letters*, 2012, **74**, 71–73.

[60] Y. Dong, J. Shao, C. Chen, H. Li, R. Wang, Y. Chi, X.Lin, G.Chen, *Carbon*, 2012, **50(12)**, 4738-43.

[61] Q. Mei, K. Zhang, G. Guan, B. Liu, S. Wang, Z. Zhang, *Chem.Commun*, 2010, **46(39)**, 7319-21.

[62] C. Galande, A. D. Mohite, A. V. Naumov, W. Gao, L. Ci, A. Ajayan, H. Gao, A. Srivastava, R. B. Weisman, P. M. Ajayan, *Sci. Rep*., 2011, **1(85)** 1.

[63] X-F. Zhang, X. Shao, S. Liu, *J. Phys. Chem. A*, 2012, **116**, 7308-7313.

[64] D. Kozawa, Y. Miyauchi, S. Mouri, K. Matsuda, *J. Phys. Chem. Lett.*, 2013, **4**, 2035-2040

[65] B. Konkena, S. Vasudevan, *J. Phys. Chem.Lett.*, 2014, **5**, 1-7

[66] P. Dutta, D. Nandi, S. Datta, S. Chakraborty, N. Das, S. Chatterjee, U. C. Ghosh, A. Halder, *J. Lumin.* 2015,**168**, 269-275.

[67] J. Shang, L. Ma, J. Li, W. Ai, T. Yu, G. G. Gurzadyan, *Sci. Rep.*, 2012, **2(792)**, 1–8

[68] A.L. Exarhos, M.E. Turk, J.M. Kikkawa, *Nano Lett*, 2013, **13(2)**, 344-349.

[69] C.T.G. Smith, R.W. Rhodes, M.J. Beliatis, K. D. I. Jayawardena, L.J. Rozanski, C. A. Mills, S. R.P. Silva, *Applied Physics Letters*, 2014. **105(7)**, 073304.

[70] S. Shi, V. Sadhu, R. Moubah, G. Schmerber, Q. Bao, S. R.P. Silva, *Journal of Materials Chemistry C*, 2013, **1(9)**, 1708-1712.

[71] S. Borini, R. White, D.Wei, M.Astley, S. Haque, E. Spigone, N. Harris, J. Kivioja, T.Ryhänen, *ACS Nano*, 2013, **7(12)**, 11166-11173.

[72] Y. Yang, A. M.Asiri, Z.Tang, D. Du, Y. Lin, *Materials Today*, 2013, **16(10)**, 365-373.

[73] S. J.Cheng, H.Y. Chiu, P. V.Kumar, K. Y.Hsieh, J. W.Yang, Y. R. Lin, Y. C.Shen G.Y. Chen, *Biomaterials Science*, 2018. **6**(4), 813-819.

[74] M. Rogala, I. Wlasny, P. Dabrowski, P. J. Kowalczyk, A. Busiakiewicz, W. Kozlowski, L. Lipinska, J. Jagiello, W. Strupinski, A. Krajewska, Z. Sieradzki, I. Krucinska, M. Puchalski, E. Skrzetuska, Z. Klusek, *Applied Physics Letters*, 2015, **106**(4), 041901.

[75] K. Erickson, R. Erni, Z. Lee, N. Alem, W. Gannett, A. Zettl, *Adv. Mater*, 2010, **22**, 4467-4472.

[76] K.P. Loh, Q. Bao, G. eda, M. Chhowalla, *Nature Chemistry,* 2010, **2**, 1015-1024.

[77]S. K. Cushing, M. Li, F. Huang, N. Wu, *ACS Nano*, 2014, **8**, 1002–1013.

[78]M. Li, S. K. Cushing, X. Zhou, S. Guoc, N. Wu, *J. Mater. Chem.*, 2012, **22**, 23374–23379.

[79] R.H. Thomas, C. Valles, R.J. Young, I.A. Kinloch, N. R. Wilson, J.P. Rourke, *J. Mater. Chem. C*, 2013, **1**, 338-342.

[80] S. Ozcan, S. Vempati, A. Cirpan, T. Uyar, *Phys. Chem. Chem. Phys*, 2018, **20**, 7559-7569.

[81] X. F. Zhang, S Liu, X. Shao, *J. Lumin.*, 2013, **136**, 32-37.

[82] H. Yu, B. Zhang, C. Bulin, R. Li , R. Xing, *Scientific Reports*, 2016. **6**, 36143.

[83] J. Shen, Y.Hu, M. Shi, X. Lu, C. Qin, C. Li, M. Ye, *Chemistry of Materials,* 2009. **21(15)**, 3514-3520.

[84] K. S. Subrahmanyam, P. Kumar, A. Nag, C. N. R. Rao. *Solid State Communications*, 2010. **150**(37–38) 1774- 177.

[85] J. L. Chen, X.P. Yan, *Journal of Materials Chemistry*, 2010. **20(21)**, 4328-4332.

[86] C. H. Lucas, A.J. Peinado, J. D.L. González, M. L.R.Cervantes, R.M.M. Aranda, *Carbon*, 1995, **33**(11),1585-1592.

[87] S. Stankovich, R.D. Piner, S.B.T Nguyen, R.S. Ruoff, *Carbon*, 2006, **44(15),** 3342-3347.

[88] T. Cassagneau, F. Guérin, J.H. Fendler, *Langmuir*, 2000. **16(18)**, 7318-7324.

[89] D.C. Marcano, D. Kosynkin, J.M. Berlin, A. Sinitskii, Z. Sun, A. Slesarev, L.B. Alemany, W. Lu, J.M. Tour, *ACS Nano*, 2010, **4(8)**, 4806-4814.

[90] A. Naumov, F. Grote, M.Overgaard, A. Roth, C.E. Halbig, K. Nørgaard, D.M. Guldi, S. Eigler, *Journal of the American Chemical Society*, 2016. **138(36)**, 11445-11448.

[91] M.T. Hasan, B.J. Senger, P. Mulford, C. Ryan, H. Doan, Z. Gryczynski, A.V. Naumov, *Nanotechnology*, 2017, **28**(6), 065705.

[92] N. Lu, Y. Huang, H. Li, Z. Li, J. Yang, *The Journal of Chemical Physics*, 2010, **133(3)**, 034502.

[93] A.V. Naumov, *Fundamentals and Applications, Wiley: Oxford*, 2016, 136-155.

[94] A. Neogi, S. Karna, R. Shah, U. Phillipose, J. Perez, R. Shimadac, Z. M. Wang, *Nanoscale*, 2014, **6(19)**, 11310-11315.

[95] F. Liu, M. Ho, J. Hyun, D. H. Hyung, K. Y. Hoon, C. Tae, *Adv Mater*, 2013.**25**. 3657-3662.

[96] A. Kundu, R.K. Layek, A.K. Nandi, *Journal of Materials Chemistry*, 2012, **22(16)**, 8139-8144.

[97] F. Yang, M. Zhao, Z. Wang, H. Ji, B. Zheng, D. Xiao, L. Wu Y. Guo, *RSC Advances*, 2014, **4(102)**, 58325-58328.

[98] X. Wan, Y. Huang, Y. Chen, *Accounts of Chemical Research*, 2012, **45(4)**, 598-607.

[99] S.S. Li, K.H. Tu, C.C. Lin, C.W. Chen, M. Chhowalla, *ACS Nano*, 2010, **4(6)**, 3169-3174.

[100] D. Sharma, S. Kanchi, M.I. Sabela, K. Bisetty, *Arabian Journal of Chemistry*, 2016, **9(2)**, 238-261.

[101] S. J. Zhu, S. J. Tang, J. H. Zhang, B. Yang, *Chem. Commun*, 2012, **48**, 4527–4539.

[102] M. A. Sk, A. Ananthanarayanan, L. Huang, K. H. Lim, P. Chen, *J. Mater. Chem. C* 2014, **2**, 6954–6960.

[103] X. Li, X. Wang, L. Zhang, S. Lee, H. Dai, *Science*, 2008, **319**, 1229-32.

[104] D. Pan, J. Zhang, Z. Li, M. Wu, *Adv Mater*, 2010, **22(6)**, 734-8.

[105] Y. Li, Y. Hu, Y. Zhao, G. Shi, L. Deng, Y. Hou, L. Quo, *Adv Mater*, 2011, **23(6)**, 776-80.

[106] S. Zhu, J. Zhang, C. Qiao, S. Tang, Y. Li, W. Yuan, B. Li, L. Tian, F. Liu, R. Hu , H. Gao, H. Wei, H. Zhang, H. Sun, B. Yang, *Chem Commun*, 2011,**47(24)**, 6858-60.

[107] H. Li, X. He, Z. Kang, H. Huang, Y. Liu, J. Liu, S. Lian, C.H. Tsang, X. Yang, S.T. Lee, *Angew Chem, Int Ed*, 2010, **49(26)**, 4430-4.

[108] S. Kim, S.W. Hwang, M.K. Kim, D.Y. Shin, D.H. Shin, C.O. Kim, *ACS Nano,* 2012, **6(9)**, 8203-8208.

[109] J. Shen, Y. Zhu, C Chen, X Yang, C. Li., *Chem Commun*, 2011, **47(9)**, 2580-2582.

[110] H. Chakraborti, S Sinha, S. Ghosh, S.K. Pal, *Mater Lett.*, 2013, **97**, 78-80.

[111] S. Kim, D.H. Shin, C.O. Kim, S.S. Kang, J. M. Kim, S.H. Choi, L.H. Jin, Y. Hoon Cho, S. W.Hwang, C. Sone, *Appl Phys Lett*, 2012,**101**, 163103.

[112] Z. Liu, J. T. Robinson, X. Sun, H. Da, *J. Am. Chem. Soc***,** 9 2008, **130(33)**, 10877.

[113] Q. Li, Y. Wang, G. Yu, Y. Liu, K. Tang, C. Ding, H. Chen, S. Yu, *Nanoscale,* 2019, **11**, 20903–20909.

[114] C. Lin, G. Xi, T. Li, X. Wang, *Chen Appl Nanosci*, 2017, **7**, 723–730.

[115] D. Dinda, A. Gupta, B. K. Shaw, S. Sadhu, S. K. Saha, *ACS Appl. Mater. Interfaces*, 2014, **6**, 10722−10728.

[116] Q. Liu, B Guo, Z. Rao, B. Zhang, J.R. Gong, *Nano Lett*, 2013, **13(6)**, 2436-41.

[117] D. Wang, L. Wang, X. Dong, Z. Shi, J. Jin, *Carbon*, 2012, **50(6)**, 2147-54.

[118] Y. Dong, G. Li, N. Zhou, R. Wang, Y. Chi, G. Chen, *Analytical Chemistry*, 2012, **84(19)**, 8378-82.

[119] L. Fan, Y. Hu, X. Wang, L. Zhang, F. Li, D. Han, *Talanta* 2012, **101**, 192-197.

[120]H. Sun, N. Gao, L. Wu, J. Ren, W. Wei, X. Qu., *European Journal,* 2013,**19(40)**, 133628.

[121] H. Zhao, Y. Chang, M. Liu, S. Gao, H. Yu, X. Quan, *Chem Commun*, 2013, **49(3)**, 2346.

[122] X. Ran, H. Sun, F. Pu, J. Ren, X. Qu, *Chem Commun,* 2013, **49(11)**, 1079-81.

[123] J.M. Bai, L. Zhang, R.P. Liang, J.D. Qiu, *A European Journal*, 2013, **19(12)**, 3822-6.

[124] Y.H. Li, L. Zhang, J. Huang, R.P. Liang, J.D. Qiu, *Chem Commun*, 2013, **49(45)**, 5180-5182.

[125] J.J. Liu, X.L. Zhang, Z.X. Cong, Z.T. Chen, Yang H-H, G.N. Chen, *Nanoscale*, 2013, **5(5)**, 1810-5.

[126] D. Dinda, B. K.Shaw, S. K. Saha, *ACS Applied Materials & Interfaces*, 2015, **7(27)**, 14743-14749

[127] V. Gupta, N. Chaudhary, R. Srivastava, G.D. Sharma, R. Bhardwaj, S. Chand, *J Am Chem Soc,* 2011, **133(26)**, 9960-9963.

[128] L. Tang, R. Ji, X Cao, J Lin, H. Jiang, X. Li, *ACS Nano*, 2012, **6(6)**, 5102-5110.

[129] D.I. Son, B.W. Kwon, D.H. Park, W.S. Seo, Y. Yi, B. Angadi, *Nat Nano*, 2012, **7(7)**, 465-471.

[130] C.M. Luk, L.B. Tang, W.F. Zhang, S.F. Yu, K.S. Teng, S.P. Lau, *J Mater Chem*, 2012, **22(42)**, 22378-22381.